

An epidemic model considering multiple factors based on multilayer

Yue-Yue Zheng(郑月月), Zhi-Ping Wang(王志平), Ya-Nan Sun(孙雅楠), Shi-Jie Xie(谢仕杰), and Lin Wang(王琳)
Citation: Chin. Phys. B, 2025, 34 (**10**): 100201. DOI: 10.1088/1674-1056/add50c
http://cpb.iphy.ac.cn; http://iopscience.iop.org/cpb

What follows is a list of articles you may be interested in

Global dynamics and optimal control of SEIQR epidemic model on heterogeneous complex networks

Xiongding Liu(柳雄顶), Xiaodan Zhao(赵晓丹), Xiaojing Zhong(钟晓静), and Wu Wei(魏武)
Chin. Phys. B, 2025, 34 (**6**): 060203. DOI: 10.1088/1674-1056/adc082

Finite-time decentralized event-triggered state estimation for coupled neural networks under unreliable Markovian network against mixed cyberattacks

Xiulin Wang(汪修林), Youzhi Cai(蔡有志), and Feng Li(李峰)
Chin. Phys. B, 2024, 33 (**11**): 110207. DOI: 10.1088/1674-1056/ad7e9a

Stochastic modeling and analysis of hepatitis and tuberculosis co-infection dynamics

Sayed Murad Ali Shah, Yufeng Nie(聂玉峰), Anwarud Din, Abdulwasea Alkhazzan, and Bushra Younas
Chin. Phys. B, 2024, 33 (**11**): 110203. DOI: 10.1088/1674-1056/ad7afa

Impact of different interaction behavior on epidemic spreading in time-dependent social networks

Shuai Huang(黄帅), Jie Chen(陈杰), Meng-Yu Li(李梦玉),Yuan-Hao Xu(徐元昊), and Mao-Bin Hu(胡茂彬)
Chin. Phys. B, 2024, 33 (**3**): 030205. DOI: 10.1088/1674-1056/ad147f

Intervention against information diffusion in static and temporal coupling networks

Yun Chai(柴允), You-Guo Wang(王友国), Jun Yan(颜俊), and Xian-Li Sun(孙先莉)
Chin. Phys. B, 2023, 32 (**9**): 090202. DOI: 10.1088/1674-1056/acb9f4

An epidemic model considering multiple factors based on multilayer hypernetworks

Yue-Yue Zheng(郑月月)[1], Zhi-Ping Wang(王志平)[1,†], Ya-Nan Sun(孙雅楠)[1], Shi-Jie Xie(谢仕杰)[1], and Lin Wang(王琳)[2,‡]

[1] *School of Science, Dalian Maritime University, Dalian* 116026, *China*
[2] *Department of Respiratory and Critical Care Medicine, Institute of Respiratory Diseases, The First Affiliated Hospital of Dalian Medical University, Dalian* 116011, *China*

(Received 3 April 2025; revised manuscript received 4 May 2025; accepted manuscript online 7 May 2025)

The outbreak of COVID-19 in 2019 has made people pay more attention to infectious diseases. In order to reduce the risk of infection and prevent the spread of infectious diseases, it is crucial to strengthen individual immunization measures and to restrain the diffusion of negative information relevant to vaccines at the opportune moment. This study develops a three-layer coupling model within the framework of hypernetwork evolution, examining the interplay among negative information, immune behavior, and epidemic propagation. Firstly, the dynamic topology evolution process of hypernetwork includes node joining, aging out, hyperedge adding and reconnecting. The three-layer communication model accounts for the multifaceted influences exerted by official media channels, subjective psychological acceptance capabilities, self-identification abilities, and physical fitness levels. Each level of the decision-making process is described using the Heaviside step function. Secondly, the dynamics equations of each state and the prevalence threshold are derived using the microscopic Markov chain approach (MMCA). The results show that the epidemic threshold is affected by three transmission processes. Finally, through the simulation testing, it is possible to enhance the intensity of official clarification, improve individual self-identification ability and physical fitness, and thereby promote the overall physical enhancement of society. This, in turn, is beneficial in controlling false information, heightening vaccination coverage, and controlling the epidemic.

Keywords: multilayer hypernetworks, information diffusion, immunization behavior, epidemic spreading

PACS: 02.50.Ga, 45.05.+x, 87.23.Kg, 64.60.aq

DOI: 10.1088/1674-1056/add50c **CSTR:** 32038.14.CPB.add50c

1. Introduction

For an extended period, various epidemic events have brought heavy impacts on individual physical and mental health, social security, and even the global economy.[1,2] The rapid development of the Internet makes global information spread indiscriminately,[3,4] and the structure of social networks becomes more and more complex. Consequently, it is crucial to utilize the dynamic network of multi-level interactions to explore the epidemic transmission mechanism more thoroughly, thereby controlling and preventing epidemic outbreaks.

Concerning epidemic transmission, Kermack *et al.* initially employed mathematical models to derive the dynamic equations and thresholds of epidemic dissemination, and first proposed the infectious disease model.[5,6] Later, experts proposed various more optimized propagation models on this basis. Among them, people have found that the spread of information in the network has a very big impact on the diffuse of the epidemic.[7–11] Specifically, Huang *et al.*[12] explored the role of knowledge infiltration in the two-layer network of information spreading and epidemic dissemination, and concluded that knowledge permeation can obviate rumours and outbreak of disease. Zhou *et al.*[13] proposed a double-layer dynamic coupling propagation model that considers individual mobility for information diffusion and epidemic transmission, revealing that epidemic transmission is to some extent influenced by the mechanism of the epidemic itself, individual mobility, and information diffusion. Li *et al.*[14] discussed the impact of multi-information dissemination and indirect touching on the expansion of the pandemic by combining individual conformity psychology, prevention costs, and risk perception within a duallayer network framework.

Certainly, the spread of the epidemic is not only influenced by the diffusion of information, but also closely related to immunization activities such as vaccination. Numerous researchers have investigated factors related to the implications of vaccination on epidemic transmission, such as vaccination costs,[15–18] vaccine risk perception,[19] vaccination strategies,[20–22] and multiple doses of vaccination.[23] Among them, Li *et al.*[24] used the SIRV-UAU coupling network to analyze the effect of individual heterogeneity represented by social differences on the epidemic and vaccine harmony, as

†Corresponding author. E-mail: wzp@dlmu.edu.cn
‡Corresponding author. E-mail: 1015132938@qq.com

© 2025 Chinese Physical Society and IOP Publishing Ltd. All rights, including for text and data mining, AI training, and similar technologies, are reserved.

well as the impact of subjective psychological perception on the evolutionary dynamics of vaccine administration, taking into account factors such as social reinforcement, forgetting mechanism and incomplete vaccination, and observed that enhancing social reinforcement and initial protection can help upgrade vaccination balance. Meng *et al.*[25] explored how evolving individual vaccination strategies influence infectious disease spread by implementing two distinct rules for updating vaccination strategies: a local strategy update rule based on return comparisons with a single random neighbour and a global update strategy based on return comparisons with the social average. The results suggest that updating personal vaccination strategies is more conducive to reducing the eventual epidemic size.

The above studies only focused on the interplay of information diffusion or vaccination behaviors on epidemic transmission, or only discussed the influence of different information propagations on vaccination.[26] However, it is essential to recognize that information diffusion, vaccination, and epidemic transmission are interconnected processes. Due to errors in the production and use of vaccines and other immunization measures, the availability of immunization is reduced, resulting in individuals' disappointment with vaccines and even wantonly dissemination of adverse vaccine-related information. The spread of negative messages could make individuals afraid of taking vaccines and other behaviors, consequently reducing the vaccination coverage rate in society. The fewer individuals who adopt immune behavior, the higher the risk of epidemic infection, which makes epidemic prevention and control more difficult. Hence, there is a need to probe the combined effects of contrary arguments related to immunization steps and the adoption of immunization behavior on epidemic transmission.

In addition, studies on the effect of information diffusion[27–29] or vaccination[31,32] on epidemic transmission have focused on complex networks. With the increasing complexity of social networks, an individual has multiple social circles, and the friends in each social circle are associated with other groups in reality or on the Internet. The complex networks based only on ordinary graphs have limitations on the current research. The hypernetwork that can contain any number of nodes and different types of subnets is more conducive to depicting the real-life network topology and dynamic evolution.[33,34] Consequently, the use of hypernetwork theory to describe information transmission in dynamic social hypernetwork[35] and epidemic dissemination dynamics[36,37] is closer to reality. On the basis of above discussion, we build a three-layer super network model, which delved into the interaction between bad immune behavior-related remarks, adoption of immune-related actions, and plague transmission. This dissertation has the following major contributions:

(i) In consideration of the high-order correlation of individuals within the network, this paper constructs a three-layer coupling UBU–$NV_{\rm E}V_{\rm I}V_{\rm E}$–$SIS$ dynamic multilayer hypernetworks propagation model. The evolution of the dynamic hypernetwork includes node entry, aging, hyperedge addition, and reconnection.

(ii) The model's first layer represents the dissemination of negative information related to immunization measures, the second layer expresses the transmission of immunization behavior, and the third layer describes the spread of epidemic.

(iii) The impact of official media, personal self-identification ability, subjective acceptance capability, and physical quality on the whole evolutionary processes is considered. And the Heaviside jump function is introduced to depict the decision–acceptation procedure.[38]

(iv) The dynamics equations in each state and prevalence threshold are obtained by using MMCA. and the validity of the model is verified, with some suggestions being put forward regarding epidemic prevention and control.

The framework of the rest of this paper is arranged as follows: The second part presents the hypernetwork evolution processes and the three-layer coupling model. The third part is analyzed theoretically by MMCA, the dynamic equation is obtained and the prevalence threshold is derived. The fourth part analyzes the model by doing lots of numeric emulation experiments. Lastly, we sum up the study of this paper and give a preview of further researches.

2. Model description

In this section, the initial social network's construction steps are described, including the three hypernetwork evolution rules. Then, the coupled dynamic process of the proposed UBU–$NV_{\rm E}V_{\rm I}V_{\rm E}$–$SIS$ model is explained in detail.

2.1. Dynamic evolution model

The concept and theory of hypergraphs is a generalization of ordinary graphs. Let $V=\{v_1,v_2,\ldots,v_n\}$ be a non-empty and finite set, and $E=\{e_1,e_2,\ldots,e_m\}$, $e_i=\{v_{i1},v_{i2},\ldots,v_{ij}\}$, $(v_{ik}\in V,\ k=1,2,\ldots,j)$, be a family of subsets of V. The pair $H=\langle V,E\rangle$ is called a hypergraph, where the element $v_1,v_2,\ldots,v_n$ is the node of the hypergraph, and the e_i $(i=1,2,\ldots,m)$ is the hyperedge of the hypergraph. In a hypergraph, if there exists a hyperedge that encompasses two nodes, the two nodes are said to be adjacent. Suppose that $\Omega=(V,E)$ is a finite hypergraph and G is a map from $T=[0,+\infty]$ into Ω. For any given $5\geq 0$, $G(t)=(V(t),E(t))$ is a finite hypergraph. A hypernetwork $\{G(t),t\in T\}$ represents a collection of hypergraphs.[39]

The hyperdegree of node v_j is the number of hyperedges containing it, denoted by $h_j=\sum_{i=1}^{m}c_{ij}$, where c_{ij} is the element in row i and column j of the incidence matrix

$C = (c_{ij})_{m\times n}$, $c_{ij} = 1$ signifies the inclusion of node v_i in hyperedge e_i, otherwise, $c_{ij} = 0$.

In the context of social networks, whether virtual or physical, individuals establish new connections based on diverse topics. The dissolution of these social connections is driven by the absence of shared interests or the cessation of interaction. Individuals transition to new social groups and forge new relationships, thereby continually reshaping their social networks. Furthermore, the social network perpetually experiences a steady influx of new individuals, who join social groups to participate in new topics. Conversely, there are also individuals who opt to disengage from ongoing topic discussions within the network. This dynamic process of information diffusion is a hallmark of social networks. In accordance with the above situation, we represent the evolution of social networks as follows: (i) Individuals build new social groups around new topics. (ii) The termination of a topic results in a new social group forming. (iii) New individuals join the social group for discussion, and those who lose interest withdraw.

Considering that individuals with strong social abilities will have greater influence, the hyperdegree preferential attachment mechanism shown below is used here for social selection between nodes:

$$W_j(t,t_i) = \frac{h_j(t,t_i)+1}{\sum_{i,j=1}[h_j(t,t_i)+1]}, \tag{1}$$

where t_i denotes the time when the i-th batch of nodes enters into the network, $h_j(t,t_i)$ presents the hyperdegree of the j-th node of the i-th batch at moment t, and $W_j(t,t_i)$ presents the probability of being selected of the j-th node of the i-th batch at moment t.

The initial social network is constructed as follows:

Step 1 Initialization

The initial network is constituted by N_0 nodes and a hyperedge containing N_0 nodes.

Step 2 Growth

At each time step, one of the following three dynamic evolution rules must occur.

(S1) New hyperedges are added with a probability of p.

Randomly select a node in the network that is encircled by a new hyperedge along with v existing nodes, totally m new hyperedges are constructed with no repetitive hyperedges. The selection rule obeys the hyperdegree preferential attachment mechanism in Eq. (1).

(S2) Hyperedges are reconnect with a probability of q.

A node v_i and one of its hyperedges e_i are randomly selected, and e_i is subsequently deleted. Following Eq. (1), the existing v nodes, along with the node i, are encircled by a new hyperedge e_i'. This process is repeated m times, ensuring that no duplicate hyperedges are created.

(S3) New node batches are added and aging nodes are deleted with a probability of $1-p-q$.

When a new batch with m_1 nodes is added to the network at time t, these new nodes and v previously existing nodes are encircled by a new hyperedge. The removal of existing nodes adheres to the node aging rule. Specifically, the earlier a node is introduced into the system, the greater the likelihood of its removal.

Step 3 Repeat

Repeat Step 2 until the network size reaches the preset value.

The dynamic network evolution process is shown schematically in Fig. 1. The meaning of the initial structure parameters of the network and the values taken are shown in Table 1. These settings are applied in all subsequent experiments.

In social networks, nodes represent individuals, and hyperedges express social circles between humans. It is clear that immune behavior and disease transmission must be accompanied by information interactions. Therefore, it is assumed here that the dynamic evolution of the network in the immune behavior layer and disease transmission layer also satisfies the above evolutionary rules.

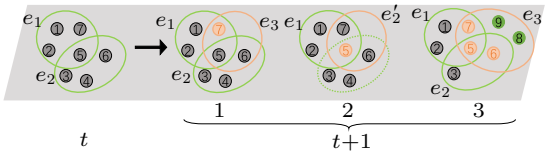


Fig. 1. Graphical representation of the dynamic evolution process of the hypernetwork. At time $t+1$, case 1 represents the addition of hyperedges (randomly choosing node v_7 and existing nodes v_5, v_6 to form a new hyperedge e_3). Case 2 represents hyperedge reconnection (randomly choosing node v_5 and the hyperedge e_2 containing it, disconnecting e_2, v_5 and v_6, v_7 to reconstruct the hyperedge e_2'). Case 3 represents the addition and removal of nodes (the new node batch containing nodes v_8, v_9 and the existing nodes v_5, v_6, v_7 form the new hyperedge e_3 and node v_4 exits).

Table 1. The meanings and values of initial network structure parameters.

Parameters	Meaning of the parameters	Values
p	probability of adding a new hyperedge	0.3
q	probability of reconnecting the hyperedge	0.25
m	number of hyperedges added or rewired	2
m_1	number of new nodes added	5
m_2	number of existing nodes removed	1
v	number of original nodes selected to form new hyperedges	5

2.2. Three-layer coupling UBU–$NV_EV_IV_E$–SIS model

In this section, we propose a three-layer interaction hypernetwork as a modeling framework for understanding coupled dynamic processes, which involve information diffusion, immune behavior, and epidemic transmission, as shown in Fig. 2. In the three-layer multiplexed networks, the nodes correspond one by one (that is, the nodes quantity in three-layer network is uniform), and that each layer of the multilayer hypernetworks has different connectivities.

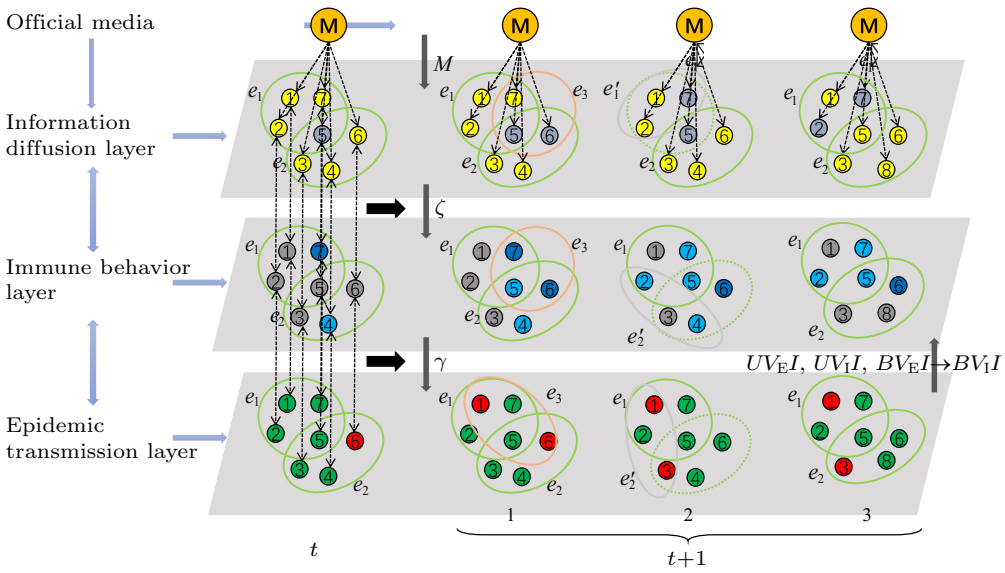


Fig. 2. Schematic diagram of model evolution mechanism. The information dissemination layer has two node statuses: Unbelieving (yellow) and believing (purple). The immune behavior layer has three node statuses: non-vaccinated (gray), vaccinated effectively (blue), and vaccinated inefficiently (navy). The epidemic transmission layer has two node statuses: susceptible (green) and infected (red). Cases 1, 2, 3 at time $t+1$ represent 1, 2, 3 of the hypernetwork dynamic evolution rules mentioned in Subsection 2.1, respectively.

Assumption 1 The first layer, termed the information dissemination layer, is characterised by the propagation path of negative information within the social network, as depicted by the network topology. This layer employs the UBU (unbelieving–believing–unbelieving) model to illustrate the propagation of negative information. The negative messages mainly refer to those related to immunization measures like vaccination (sequelae, by-effects, *etc*.) on online social networks. Among them, the person with U-state does not know or believe the negative information, while the B-state individual is aware of the negative message, believes and disseminates it. Here, individuals' choice, whether believe negative information or not, is mainly influenced by their self-discriminating ability, that is, when individuals have a high ability to distinguish between true and false message, they have a higher belief threshold for unconfirmed information and will not easily believe unfounded one. On the contrary, it is easy to believe vague information, so that it is easy to be misled by wrong information, thereby increasing infection risks. Let the individual's self-distinguishing ability be s_i $(0 \le s_i \le 1)$ and assume it follows the normal distribution $G_1(s_i) \sim N(\mu_1, \sigma_1)$[38] to describe the heterogeneity of individual discriminative ability, where μ_1 represents the mean self-distinguishing capability of the entire group in the network, and σ_1 denotes the fluctuation amplitude of the difference in the group's self-discriminating ability. At the same time, considering that individuals are likely to be affected by people around them and thus taking herd actions, this part uses Heaviside step function to represent the state transformation probability of the information dissemination layer. That is, when $x > 0$, $H(x) = 1$, people choose to believe negative information. Otherwise, $H(x) = 0$, the individual does not choose to believe it. Therefore, hypothesizing the possibility of U-state people believing the negative messages is

$$\lambda_i(t) = \lambda H\left(\frac{\sum_{j=1} P_j^B(t)}{k_i(t)} - s_i\right), \tag{2}$$

where λ refers to the initial information propagation rate, $\sum_{j=1} P_j^{mB}(t)/k_i(t)$ represents the proportion of nodes in status B among neighbours v_j around node v_i at time t, $k_i(t)$ represents the number of nodes adjacent to v_i at time t, and $P_j^B(t)$ refers to the chance of individual v_j believing in negative information (being in status B) at time t. When $s_i = 0$, it indicates that the individual has no self-distinguishing ability at all and is completely affected by the group behavior of the surrounding environment. When $s_i = 1$, individuals totally influenced by their highest self-distinguishing ability. Only when $\sum_{j=1} P_j^B(t)/k_i(t) > s_i$, will the individual believe the negative information with possibility λ.

In state B, individuals will forget the information or gradually wake up from the misleading information with a certain probability δ, and then change to state U to choose not to believe the negative information.

Moreover, considering that in real life, timely clarification of unfounded remarks by authoritative media such as official accounts will play a great role in curbing the spread of rumors, let us introduce officially authorized mass media here,[12] which is associated with all points of the information dissemination layer. When the correct message is released by the official media, individuals in state B will accept the clarified information with probability M and change to state U.

Assumption 2 The second layer, termed the immune behavior layer, is characterised by the propagation path of

the immune measures in the current physical contact, as depicted by the network topology. This layer employs the $NV_{\rm E}V_{\rm I}V_{\rm E}$ (nonvaccinated-vaccinated–vaccinated ineffectively-vaccinated)[4] model to illustrate the propagation of immune behavior. The immunization measures outlined in this paper primarily address the decision-making process regarding vaccination. The nodes in state N have not yet taken the vaccination behaviors, and individuals in state $V_{\rm E}$ indicate that they have been vaccinated, and $V_{\rm I}$-state nodes refer to an individual who has adopted immune conduct but unfortunately remains infected. We consider whether choosing to take immunization measures is related to the inner acceptance of individuals. If individuals have a fear of vaccination, that is, their inner acceptability of vaccination is low, then the threshold of vaccination will be high and the possibility of choosing immunization measures will be low, otherwise the opposite. Here, we suggest that the more people believe in negative information, the more it affects people's adoption of immune behaviors. Once individuals realize and believe immune-related negative information, their willingness to vaccinate is likely to be greatly reduced. Thereby, we assume that θ_i is the acceptance threshold of node v_i, θ is the doorsill of immune action of individuals that is not affected by other factors $(0 \leq \theta \leq 1)$, and then the acceptance doorsill of individuals in state B is $\theta_i^B = \theta$. The attenuation factor ζ $(0 \leq \zeta \leq 1)$ is introduced to depict the impact of negative information related to immune measures on individuals' aspiration to take immune behaviors, and the acceptance doorsill of individuals in state U is $\theta_i^U = \zeta\theta$. At the same time, considering that people will follow the effect of the behaviors trend of their neighbors, here we believe that individuals' deed of taking immune measures belongs to a process of adopting decision-making, which is described by the Heaviside step function. Set the probability of immunization for unvaccinated nodes as

$$\alpha_i^X(t) = \alpha H\left(\frac{\sum\limits_{j=1} P_j^V(t)}{k_i(t)} - \theta_i^X\right), \tag{3}$$

where, $X \in \{U, B\}$ and α refers to the initial probability of taking action, $\sum_{j=1} P_j^V(t)/k_i(t)$ represents the proportion of individuals taking immune behaviors in the neighbor v_j of node v_i at time t, $k_i(t)$ represents the number of nodes adjacent to v_i at time t, and $P_j^V(t) = P_j^{V_{\rm E}}(t) + P_j^{V_{\rm I}}(t)$ refers to the sum of probabilities of person in state $V_{\rm E}$ and state $V_{\rm I}$ at time t. As long as the proportion of vaccinated neighbors $\sum_{j=1} P_j^V(t)/k_i(t)$ is higher than the individual's inner acceptance threshold θ_i^U, people will take immune measures with probability α.

In the immune behavior layer, this paper takes into account the fact that in real life vaccinated individuals are still at risk of being infected, that is, if the vaccinated individual is infected, this means that the individual's status in the second layer changes from $V_{\rm E}$ to $V_{\rm I}$. Suppose that the probability of individual who has been immunised being infected is β^V $\left(\beta^V = \beta^{UV_{\rm E}S} + \beta^{BV_{\rm E}S}\right)$, which will be discussed in detail in Assumption 3. In addition, we think that individuals who have lost immunity may choose to re-immunize, and assume that a recovered vaccine-ineffective individual has the same probability of vaccination as an individual who has never been vaccinated.

Assumption 3 The third layer, termed the epidemic transmission layer, simulates the epidemic transmission model under the effect of negative information spreading and immune behavior through *SIS* (susceptible–infected–susceptible) model.[41]

In epidemic transmission layer, we believe that the infection situation of different individuals will be affected by individual physical fitness, and the better the physical fitness of person, the stronger the immune ability to resist diseases. Here, f_i is used to portray the heterogeneity of personal physique, and postulate that it follows the normal distribution $G_2(f_i) \sim N(\mu_2, \sigma_2)$, where μ_2 represents the average physical fitness of the entire group in the network, and σ_2 means the fluctuation amplitude of physical fitness differences in the group. Besides, the conduct of immunization measures will improve the level of personal physical fitness to a certain extent, so it is assumed that

$$f = \begin{cases} f_i, & \text{the state of } V_{\rm E}, \\ \gamma_1 f_i, & \text{the state of } V_{\rm I}, \\ \gamma_2 f_i, & \text{the state of } N, \end{cases}$$

where γ_i $(i = 1, 2)$ represents the degree of physical fitness decline of individuals who did not take immunological behaviors and immune failure. Logically, as long as immunization measures are taken, even if they are infected later, the relevant steps will still produce some antibodies in the body to some extent, so $\gamma_1 \in [0.5, 1]$, $\gamma_2 \in [0, 0.5)$. However, in order to reduce the equation, let $\gamma_1 = \gamma_2 = \gamma$, then we get

$$f = \begin{cases} f_i, & \text{the state of } V_{\rm E}, \\ \gamma f_i, & \text{the state of } V_{\rm I} \text{ or } N. \end{cases}$$

Meanwhile, the infection rate of each individual was also related to its corresponding status in information dissemination layer and immune behavior layer. If an individual believes negative message or does not adopt relevant immune behaviors, then he will reduce his alertness to approaching others, thus increasing the risk of contagion. Therefore, we assume that people who do not believe negative information will reduce φ_1 $(0 \leq \varphi_1 \leq 1)$ infection rate, and as long as individuals take immune measures (whether effective or not), the probability of infection will be reduced φ_2 $(0 \leq \varphi_2 \leq 1)$. Thus, the initial infection probabilities under different states can be ob-

tained as follows:

$$\beta^Y = \begin{cases} \beta, & \text{the state of } BNS, \\ \varphi_1\beta, & \text{the state of } UNS, \\ \varphi_2\beta, & \text{the state of } BV_{\mathrm{E}}S, BV_{\mathrm{I}}S, \\ \varphi_1\varphi_2\beta, & \text{the state of } UV_{\mathrm{E}}S, UV_{\mathrm{I}}S, \end{cases}$$

where $Y \in \{UNS, BNS, UV_{\mathrm{E}}S, BV_{\mathrm{E}}S, UV_{\mathrm{I}}S, BV_{\mathrm{I}}S\}$ and β refers to the initial probability of infection.

To simplify our model, this paper regards the influence of information as equivalent to that of immune behavior, namely $\varphi_1 = \varphi_2 = \varphi$. The initial infection probability after the simplified parameters can be obtained that

$$\beta^Y = \begin{cases} \beta, & \text{the state of } BNS, \\ \varphi\beta_i, & \text{the state of } UNS, BV_{\mathrm{E}}S, BV_{\mathrm{I}}S, \\ \varphi^2\beta_i, & \text{the state of } UV_{\mathrm{E}}S, UV_{\mathrm{I}}S. \end{cases}$$

Considering that the entire process of epidemic infection is closely related to the physical fitness of individuals and the infection of their neighbors, we believe that epidemic infection is a decision-making process, which is also expressed by the Heaviside step function. So, we can get the corresponding infection rate as follows:

$$\begin{cases} \beta_i^{BNS}(t) = \beta H\left(\frac{\sum_{j=1} P_j^{\mathrm{I}}(t)}{k_i(t)} - \gamma f_i\right), \\ \beta_i^{UNS}(t) = \beta_i^{BV_{\mathrm{I}}S}(t) = \varphi\beta H\left(\frac{\sum_{j=1} P_j^{\mathrm{I}}(t)}{k_i(t)} - \gamma f_i\right), \\ \beta_i^{BV_{\mathrm{E}}S}(t) = \varphi\beta H\left(\frac{\sum_{j=1} P_j^{\mathrm{I}}(t)}{k_i(t)} - f_i\right), \\ \beta_i^{UV_{\mathrm{E}}S}(t) = \varphi^2\beta H\left(\frac{\sum_{j=1} P_j^{\mathrm{I}}(t)}{k_i(t)} - f_i\right), \\ \beta_i^{UV_{\mathrm{I}}S}(t) = \varphi^2\beta H\left(\frac{\sum_{j=1} P_j^{\mathrm{I}}(t)}{k_i(t)} - \gamma f_i\right), \end{cases} \tag{4}$$

where, $\sum_{j=1} P_j^{\mathrm{I}}(t)/k_i(t)$ represents the proportion of individuals infected with infectious diseases in the neighbor v_j of node v_i at time t, $k_i(t)$ represents the number of nodes adjacent to v_i at time t, and $P_j^{\mathrm{I}}(t)$ refers to the probability that individuals are in state I at time t. φ denotes the infection rate attenuation factor that is not affected by information or immune behavior, $0 \le \varphi \le 1$. If an individual is infected with possibility β^Y, it is necessary to meet the requirement that the proportion of pathogenic individuals around $\sum_{j=1} P_j^{\mathrm{I}}(t)/k_i(t)$ is greater than individual constitution f.

The I state individual will be healed and back to S state with recovery rate μ.

Assumption 4 Thus, the individual states under the three-layer coupling hypernetworks can be obtained as follows: UNS, UNI, $UV_{\mathrm{E}}S$, $UV_{\mathrm{E}}I$, $UV_{\mathrm{I}}S$, $UV_{\mathrm{I}}I$, BNS, BNI, $BV_{\mathrm{E}}S$, $BV_{\mathrm{E}}I$, $BV_{\mathrm{I}}S$, $BV_{\mathrm{I}}I$. In this paper, it is assumed that once infected, vaccinated individuals will be disappointed with immunization measures and believe negative information. Hence, individuals of states $UV_{\mathrm{E}}I$, $UV_{\mathrm{I}}I$, and $BV_{\mathrm{E}}I$ will automatically change into state $BV_{\mathrm{I}}I$. Finally, there are 9 valid node states involved, which are UNS, UNI, $UV_{\mathrm{E}}S$, $UV_{\mathrm{I}}S$, BNS,

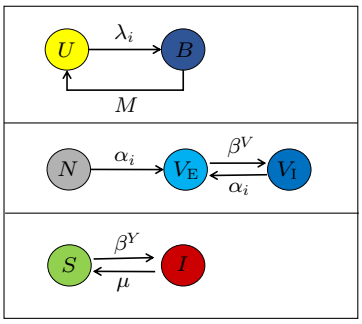


Fig. 3. Schematic diagram of transitions between states of each layer. From top to bottom, the image shows the process of spreading negative information related to immune behavior, the process of taking immunization measures, and the process of spreading epidemics.

Table 1. The definition of relevant parameters to the three-layer model.

Parameters	Definition
H	Heaviside step function
λ	initial information propagation rate
s_i	self-distinguishing ability of individual v_i
μ_1	average self-distinguishing ability of the entire group
σ_1	fluctuation amplitude of the difference in the group's self-distinguishing ability
λ_i	probability of Ustate individuals believing negative information
M	The probability of B state individuals accepting the clarified information from official mass
δ	probability of negative information forgetting
α	initial probability of taking immune action
ζ	attenuation factor of immune behavior acceptance doorsill
θ	doorsill of immune action of individuals that is not affected by other factors
α_i	The probability of immunization for unvaccinated individuals
f_i	physical fitness of individual v_i
μ_2	average physical fitness of the entire group
σ_2	fluctuation amplitude of the difference in the group's physical fitness
γ	attenuation factor of physical fitness for V_{I} or N individuals
β	initial probability of infection
β_i^Y	probability of individuals in different states being infected
φ	attenuation factor of infection rate for V_{E}, V_{I} or U individuals
μ	probability of I state individuals being healed

BNI, $BV_{\rm E}S$, $BV_{\rm I}S$, $BV_{\rm I}I$. Based on the description of the hypernetwork evolution model and the *UBU–*$NV_{\rm E}V_{\rm I}V_{\rm E}$*–SIS* model, we show the information-immune-epidemic transmission process based on the hypernetwork evolution in Fig. 3. Besides, the relevant parameters involved are defines as shown in Table 2.

3. Theoretical analysis

3.1. Dynamic network theory analysis

The total amount of super network nodes is denoted as $N(t)$. According to the dynamic evolvement mechanism of hypernetwork introduced in Subsection 2.1, we can depict the dynamic equations about hyper degree $h_j(t,t_i)$ as follows.

(i) New hyperedges are added with a probability of p

$$\frac{\partial h_j(t,t_i)}{\partial t} = pm\left\{\frac{1}{N(t)} + v\frac{h_j(t,t_i)+1}{\sum_{i,j=1}[h_j(t,t_i)+1]}\right\}. \tag{5}$$

(ii) Hyperedges are reconnect with a probability of q

$$\frac{\partial h_j(t,t_i)}{\partial t} = qm\left\{-\frac{1}{N(t)} + v\frac{h_j(t,t_i)+1}{\sum_{i,j=1}[h_j(t,t_i)+1]}\right\}. \tag{6}$$

(iii) New node batches are added with a probability of $1-p-q$

$$\frac{\partial h_j(t,t_i)}{\partial t} = (1-p-q)v\widetilde{\lambda}_1 m_1 \frac{h_j(t,t_i)+1}{\sum_{i,j=1}[h_j(t,t_i)+1]}, \tag{7}$$

where $\widetilde{\lambda}_1$ presents the entry rate of nodes, assuming that it obeys the Poisson distribution.

Combining Eqs. (5)–(7), we can get

$$\frac{\partial h_j(t,t_i)}{\partial t} = \frac{(p-q)m}{N(t)} + \left[(p+q)m+(1-p-q)\widetilde{\lambda}_1 m_1\right]v \times \frac{h_j(t,t_i)+1}{\sum_{i,j=1}[h_j(t,t_i)+1]}. \tag{8}$$

For large t, $N(t) \approx (1-p-q)\widetilde{\lambda}_1 m_1 t$, $\sum_{i,j=1}[h_j(t,t_i)+1] \approx [mp(1+v)+(1-p-q)m_1]\cdot E[N(t)]$. Let $C_1 = (1-p-q)\widetilde{\lambda}_1 m_1$, $C_2 = mp(1+v)+(1-p-q)m_1$, equation (8) can become

$$\frac{\partial h_j(t,t_i)}{\partial t} = \frac{(p-q)m}{C_1 t} + \left[(p+q)m+(1-p-q)\widetilde{\lambda}_1 m_1\right] \times v\frac{h_j(t,t_i)+1}{C_2 E[N(t)]}. \tag{9}$$

To simplify the equation, let $A = m(p-q)/C_1$, $D = \left[(p+q)m+(1-p-q)\widetilde{\lambda}_1 m_1\right]v$, we can simplify Eq. (8) as

$$\frac{\partial h_j(t,t_i)}{\partial t} = \frac{A}{t} + B\frac{h_j(t,t_i)}{C_2 E[N(t)]}. \tag{10}$$

By integrating both sides of Eq. (10) simultaneously, the hyper degree can be obtained

$$h_j(t,t_i) = \left(m_1 + \frac{A+C}{C}\right)\left(\frac{t}{t_i}\right)^C - \frac{A+C}{C}, \tag{11}$$

where

$$A = \frac{m(p-q)}{(1-p-q)\widetilde{\lambda}_1 m_1},$$

$$C = \frac{\left[(p+q)m+(1-p-q)\widetilde{\lambda}_1 m_1\right]v}{[mp(1+v)+(1-p-q)m_1](1-p-q)\widetilde{\lambda}_1 m_1}.$$

3.2. Theoretical analysis based on MMCA

Based on the three-layer *UBU–*$NV_{\rm E}V_{\rm I}V_{\rm E}$*–SIS* model regard to official media, the j-th node of the i-th batch can be in a certain state: $P_j^{UNS}(t,t_i)$, $P_j^{BNS}(t,t_i)$, $P_j^{UV_{\rm E}S}(t,t_i)$, $P_j^{BV_{\rm E}S}(t,t_i)$, $P_j^{UV_{\rm I}S}(t,t_i)$, $P_j^{BV_{\rm I}S}(t,t_i)$, $P_j^{UNI}(t,t_i)$, $P_j^{BNI}(t,t_i)$, $P_j^{BV_{\rm I}I}(t,t_i)$. They satisfy the normalization condition that the sum of the above nine probabilities is 1. Let $(a_{ijkl})_{N\times N}$, $(b_{ijkl})_{N\times N}$, and $(c_{ijkl})_{N\times N}$ be the adjacent matrix of information, behaviors, and epidemic transmission levels, separately. We record n_{ij} as the j-th node of the i-th batch, in the layer of negative information spread, if node n_{ij} and n_{kl} are interrelated, so then $a_{ijkl}=1$, or $a_{ijkl}=0$. Similarly, in the vaccination behavior layer (or epidemic propagation layer), if node n_{ij} is linked with n_{kl}, then $b_{ijkl}=1$ $(c_{ijkl}=1)$, otherwise $b_{ijkl}=0$ $(c_{ijkl}=0)$. Besides, we let $r_j(t,t_i)$ presents the probability of U-state individual n_{ij} does not believe the negative information propagated by the neighbors in the first layer at time t. $q_j^{UNS}(t,t_i)$, $q_j^{BNS}(t,t_i)$, $q_j^{UV_{\rm E}S}(t,t_i)$, $q_j^{BV_{\rm E}S}(t,t_i)$, $q_j^{UV_{\rm I}S}(t,t_i)$, and $q_j^{BV_{\rm I}S}(t,t_i)$ is used to express the chance that the individual n_{ij} in the corresponding status is not permeated by the neighbors at time t, respectively.

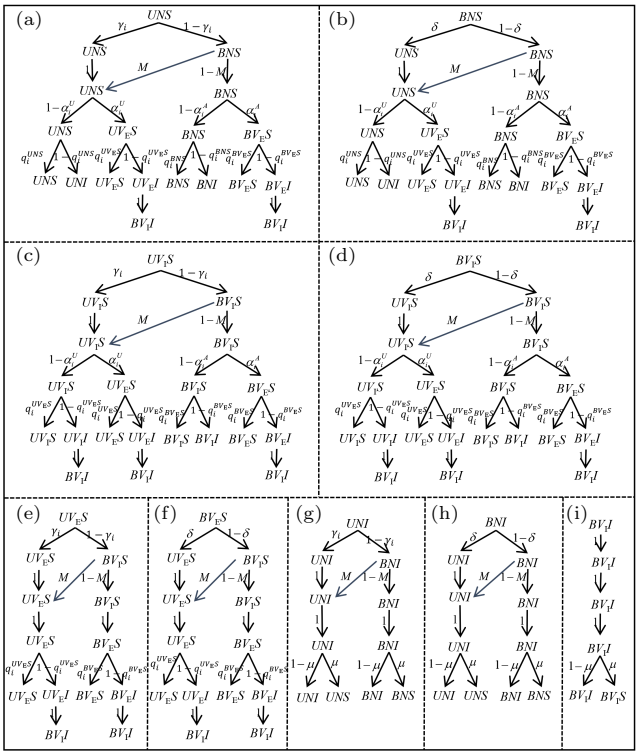


Fig. 4. Transfer probability tree of nine available statuses in the three-layer network model.

$$
\begin{aligned}
r_j(t,t_i) &= \prod_k \prod_l \left[1 - a_{ijkl} P_l^B(t,t_k)\,\lambda_j(t,t_i)\right], \\
q_j^{UNS}(t,t_i) &= \prod_k \prod_l \left[1 - c_{ijkl} P_l^{\mathrm{I}}(t,t_k)\,\beta_j^{UNS}(t,t_i)\right], \\
q_j^{BNS}(t,t_i) &= \prod_k \prod_l \left[1 - c_{ijkl} P_l^{\mathrm{I}}(t,t_k)\,\beta_j^{BNS}(t,t_i)\right], \\
q_j^{UV_{\mathrm{E}}S}(t,t_i) &= \prod_k \prod_l [1 - c_{ijkl} P_l^{\mathrm{I}}(t,t_k)\,\beta_j^{UV_{\mathrm{E}}S}(t,t_i)], \\
q_j^{BV_{\mathrm{E}}S}(t,t_i) &= \prod_k \prod_l [1 - c_{ijkl} P_l^{\mathrm{I}}(t,t_k)\,\beta_j^{BV_{\mathrm{E}}S}(t,t_i)], \\
q_j^{UV_{\mathrm{I}}S}(t,t_i) &= \prod_k \prod_l [1 - c_{ijkl} P_l^{\mathrm{I}}(t,t_k)\,\beta_j^{UV_{\mathrm{I}}S}(t,t_i)], \\
q_j^{BV_{\mathrm{I}}S}(t,t_i) &= \prod_k \prod_l [1 - c_{ijkl} P_l^{\mathrm{I}}(t,t_k)\,\beta_j^{BV_{\mathrm{I}}S}(t,t_i)], \qquad (12)
\end{aligned}
$$

where

$$
\begin{aligned}
P_l^B(t,t_k) &= P_l^{BNS}(t,t_k) + P_l^{BNI}(t,t_k) + P_l^{BV_{\mathrm{E}}S}(t,t_k) \\
&\quad + P_l^{BV_{\mathrm{E}}I}(t,t_k) + P_l^{BV_{\mathrm{I}}I}(t,t_k), \\
P_l^{\mathrm{I}}(t,t_k) &= P_l^{UNI}(t,t_k) + P_l^{BNI}(t,t_k) + P_l^{BV_{\mathrm{I}}I}(t,t_k).
\end{aligned}
$$

Then, according to Fig. 3 and Eq. (12), a state transitional probability tree can be established to announce the transfer probabilities among 9 diverse states, as figure 4 shows.

Furthermore, based on this, we can use the MMCA to establish the following transformation equations of the relevant states.[42–44]

$$
\begin{aligned}
P_j^{UNS}(t+1,t_i) &= \left\{P_j^{UNS}(t,t_i)\left[r_j(t,t_i) + (1-r_j(t,t_i))M\right] + P_j^{BNS}(t,t_i)\left[\delta + (1-\delta)M\right]\right\}\left[1-\alpha_j^U(t,t_i)\right] q_j^{UNS}(t,t_i) \\
&\quad + \left\{P_j^{UNI}(t,t_i)\left[r_j(t,t_i) + (1-r_j(t,t_i))M\right] + P_j^{BNI}(t,t_i)\left[\delta + (1-\delta)M\right]\right\}\mu, \\
P_j^{BNS}(t+1,t_i) &= \left\{P_j^{UNS}(t,t_i)\left[1-r_j(t,t_i)\right] + P_j^{BNS}(t,t_i)(1-\delta)\right\}(1-M)\left[1-\alpha_j^A(t,t_i)\right] q_j^{BNS}(t,t_i) \\
&\quad + \left\{P_j^{UNI}(t,t_i)\left[1-r_j(t,t_i)\right] + P_j^{BNI}(t,t_i)(1-\delta)\right\}(1-M)\mu, \\
P_j^{UV_{\mathrm{I}}S}(t+1,t_i) &= P_j^{UV_{\mathrm{I}}S}(t,t_i)\left[r_j(t,t_i) + (1-r_j(t,t_i))M\right]\left[1-\alpha_j^U(t,t_i)\right] q_j^{UV_{\mathrm{I}}S}(t,t_i) \\
&\quad + P_j^{BV_{\mathrm{I}}S}(t,t_i)\left[\delta + (1-\delta)M\right]\left[1-\alpha_j^U(t,t_i)\right] q_j^{UV_{\mathrm{I}}S}(t,t_i), \\
P_j^{BV_{\mathrm{I}}S}(t+1,t_i) &= P_j^{UV_{\mathrm{I}}S}(t,t_i)\left[1-r_j(t,t_i)\right](1-M)\left[1-\alpha_j^A(t,t_i)\right] q_j^{BV_{\mathrm{I}}S}(t,t_i) \\
&\quad + P_j^{BV_{\mathrm{I}}S}(t,t_i)(1-\delta)(1-M)\left[1-\alpha_j^A(t,t_i)\right] q_j^{BV_{\mathrm{I}}S}(t,t_i) + P_j^{BV_{\mathrm{I}}I}(t,t_i)\mu, \\
P_j^{UV_{\mathrm{E}}S}(t+1,t_i) &= \left\{P_j^{UNS}(t,t_i) + P_j^{UV_{\mathrm{I}}S}(t,t_i)\right\} P_j^{UNS}(t,t_i)\left[r_j(t,t_i) + (1-r_j(t,t_i))M\right]\alpha_j^U(t,t_i)\, q_j^{UV_{\mathrm{E}}S}(t,t_i) \\
&\quad + \left\{P_j^{BNS}(t,t_i) + P_j^{BV_{\mathrm{I}}S}(t,t_i)\right\} P_j^{BNS}(t,t_i)\left[\delta + (1-\delta)M\right]\alpha_j^U(t,t_i)\, q_j^{UV_{\mathrm{E}}S}(t,t_i) \\
&\quad + \left\{P_j^{UV_{\mathrm{E}}S}(t,t_i)\left[r_j(t,t_i) + (1-r_j(t,t_i))M\right] + P_j^{UV_{\mathrm{I}}S}(t,t_i)\left[\delta + (1-\delta)M\right]\right\} q_j^{UV_{\mathrm{E}}S}(t,t_i), \\
P_j^{BV_{\mathrm{E}}S}(t+1,t_i) &= \left\{\left[P_j^{UNS}(t,t_i) + P_j^{UV_{\mathrm{I}}S}(t,t_i)\right]\left[1-r_j(t,t_i)\right] + \left[P_j^{BNS}(t,t_i) + P_j^{BV_{\mathrm{I}}S}(t,t_i)\right](1-\delta)\right\}(1-M)\alpha_j^A(t,t_i)\, q_j^{BV_{\mathrm{E}}S}(t,t_i) \\
&\quad + \left\{P_j^{UV_{\mathrm{E}}S}(t,t_i)\left[1-r_j(t,t_i)\right] + P_j^{BV_{\mathrm{E}}S}(t,t_i)(1-\delta)\right\}(1-M) q_j^{BV_{\mathrm{E}}S}(t,t_i), \\
P_j^{UNI}(t+1,t_i) &= \left\{P_j^{UNS}(t,t_i)\left[r_j(t,t_i) + (1-r_j(t,t_i))M\right] + P_j^{UNS}(t,t_i)\left[\delta + (1-\delta)M\right]\right\}\left[1-\alpha_j^U(t,t_i)\right]\left[1-q_j^{UNS}(t,t_i)\right] \\
&\quad + \left\{P_j^{UNI}(t,t_i)\left[r_j(t,t_i) + (1-r_j(t,t_i))M\right] + P_j^{BNI}(t,t_i)\left[\delta + (1-\delta)M\right]\right\}(1-\mu), \\
P_j^{BNI}(t+1,t_i) &= \left\{P_j^{UNS}(t,t_i)\left[1-r_j(t,t_i)\right] + P_j^{BNS}(t,t_i)(1-\delta)\right\}(1-M)\left[1-\alpha_j^A(t,t_i)\right]\left[1-q_j^{BNS}(t,t_i)\right] \\
&\quad + \left\{P_j^{UNI}(t,t_i)\left[1-r_j(t,t_i)\right] + P_j^{BNI}(t,t_i)(1-\delta)\right\}(1-M)(1-\mu), \\
P_j^{BV_{\mathrm{I}}I}(t+1,t_i) &= \left\{P_j^{UNS}(t,t_i)\left[r_j(t,t_i) + (1-r_j(t,t_i))M\right] + P_j^{BNS}(t,t_i)\left[\delta + (1-\delta)M\right]\right\}\alpha_j^U(t,t_i)\left[1-q_j^{UV_{\mathrm{E}}S}(t,t_i)\right] \\
&\quad + \left\{P_j^{UNS}(t,t_i)\left[1-r_j(t,t_i)\right] + P_j^{BNS}(t,t_i)(1-\delta)\right\}(1-M)\alpha_j^A(t,t_i)\left[1-q_j^{BV_{\mathrm{E}}S}(t,t_i)\right] \\
&\quad + \left\{P_j^{UV_{\mathrm{I}}S}(t,t_i)\left[r_j(t,t_i) + (1-r_j(t,t_i))M\right] + P_j^{BV_{\mathrm{I}}S}(t,t_i)\left[\delta + (1-\delta)M\right]\right\}\left[1-\alpha_j^U(t,t_i)\right]\left[1-q_j^{UV_{\mathrm{I}}S}(t,t_i)\right] \\
&\quad + \left\{P_j^{UV_{\mathrm{I}}S}(t,t_i)\left[r_j(t,t_i) + (1-r_j(t,t_i))M\right] + P_j^{BV_{\mathrm{I}}S}(t,t_i)\left[\delta + (1-\delta)M\right]\right\}\alpha_j^U(t,t_i)\left[1-q_j^{UV_{\mathrm{E}}S}(t,t_i)\right] \\
&\quad + \left\{P_j^{UV_{\mathrm{I}}S}(t,t_i)\left[1-r_j(t,t_i)\right] + P_j^{BV_{\mathrm{I}}S}(t,t_i)(1-\delta)\right\}(1-M)\left[1-\alpha_j^A(t,t_i)\right]\left[1-q_j^{BV_{\mathrm{I}}S}(t,t_i)\right] \\
&\quad + \left\{P_j^{UV_{\mathrm{I}}S}(t,t_i)\left[1-r_j(t,t_i)\right] + P_j^{BV_{\mathrm{I}}S}(t,t_i)(1-\delta)\right\}(1-M)\alpha_j^A(t,t_i)\left[1-q_j^{BV_{\mathrm{E}}S}(t,t_i)\right] \\
&\quad + \left\{P_j^{UV_{\mathrm{E}}S}(t,t_i)\left[r_j(t,t_i) + (1-r_j(t,t_i))M\right] + P_j^{BV_{\mathrm{E}}S}(t,t_i)\left[\delta + (1-\delta)M\right]\right\}\left[1-q_j^{UV_{\mathrm{E}}S}(t,t_i)\right] \\
&\quad + \left\{P_j^{UV_{\mathrm{E}}S}(t,t_i)\left[1-r_j(t,t_i)\right] + P_j^{BV_{\mathrm{E}}S}(t,t_i)(1-\delta)\right\}(1-M)\left[1-q_j^{BV_{\mathrm{E}}S}(t,t_i)\right] + P_j^{BV_{\mathrm{I}}I}(t,t_i)(1-\mu). \qquad (13)
\end{aligned}
$$

As time approaches infinity, the system tends to stability, and $P_j(t+1,t_i) = P_j(t,t_i) = P_{ij}$ is applicable to any node and all states available. β_c is a crucial parameter in the epidemic spread network, and the number of individual infections is close to zero near the epidemic threshold value. Therefore, assuming $P_{ij}^{\mathrm{I}} = P_{ij}^{UNI} + P_{ij}^{BNI} + P_{ij}^{BV_{\mathrm{I}}I} = \varepsilon_{ij} \ll 1$, equation (12) might be approached as

$$\begin{aligned}
q_j^{UNS}(t,t_i) &= \prod_k \prod_l \left[1 - c_{ijkl} P_l^{\mathrm{I}}(t,t_k)\, \beta_j^{UNS}(t,t_i)\right] \\
&\approx 1 - \beta_{ij}^{UNS} \sum_k \sum_l c_{ijkl}\varepsilon_{kl}, \\
q_j^{BNS}(t,t_i) &= \prod_k \prod_l \left[1 - c_{ijkl} P_l^{\mathrm{I}}(t,t_k)\, \beta_j^{BNS}(t,t_i)\right] \\
&\approx 1 - \beta_{ij}^{BNS} \sum_k \sum_l c_{ijkl}\varepsilon_{kl}, \\
q_j^{UV_{\mathrm{E}}S}(t,t_i) &= \prod_k \prod_l \left[1 - c_{ijkl} P_l^{\mathrm{I}}(t,t_k)\, \beta_j^{UV_{\mathrm{E}}S}(t,t_i)\right] \\
&\approx 1 - \beta_{ij}^{UV_{\mathrm{E}}S} \sum_k \sum_l c_{ijkl}\varepsilon_{kl}, \\
q_j^{BV_{\mathrm{E}}S}(t,t_i) &= \prod_k \prod_l \left[1 - c_{ijkl} P_l^{\mathrm{I}}(t,t_k)\, \beta_j^{BV_{\mathrm{E}}S}(t,t_i)\right] \\
&\approx 1 - \beta_{ij}^{BV_{\mathrm{E}}S} \sum_k \sum_l c_{ijkl}\varepsilon_{kl}, \\
q_j^{UV_{\mathrm{I}}S}(t,t_i) &= \prod_k \prod_l \left[1 - c_{ijkl} P_l^{\mathrm{I}}(t,t_k)\, \beta_j^{UV_{\mathrm{I}}S}(t,t_i)\right] \\
&\approx 1 - \beta_{ij}^{UV_{\mathrm{I}}S} \sum_k \sum_l c_{ijkl}\varepsilon_{kl}, \\
q_j^{BV_{\mathrm{I}}S}(t,t_i) &= \prod_k \prod_l \left[1 - c_{ijkl} P_l^{\mathrm{I}}(t,t_k)\, \beta_j^{BV_{\mathrm{I}}S}(t,t_i)\right] \\
&\approx 1 - \beta_{ij}^{BV_{\mathrm{I}}S} \sum_k \sum_l c_{ijkl}\varepsilon_{kl}.
\end{aligned} \tag{14}$$

Combining Eqs. (13) and (14), the last expression in Eq. (13) can be simplified as follows:

$$\begin{aligned}
\mu\varepsilon_{ij} = {} & \left\{P_{ij}^{UNS}[r_{ij} + (1-r_{ij})M] + P_{ij}^{BNS}[\delta + (1-\delta)M]\right\}\left(1-\alpha_{ij}^{U}\right)\beta_{ij}^{UNS}\sum_k\sum_l c_{ijkl}\varepsilon_{kl} \\
& + \left[P_{ij}^{UNS}(1-r_{ij}) + P_{ij}^{BNS}(1-\delta)\right](1-M)\left(1-\alpha_{ij}^{A}\right)\beta_{ij}^{BNS}\sum_k\sum_l c_{ijkl}\varepsilon_{kl} \\
& + \left\{P_{ij}^{UNS}[r_{ij} + (1-r_{ij})M] + P_{ij}^{BNS}[\delta + (1-\delta)M]\right\}\alpha_{ij}^{U}\beta_{ij}^{UV_{\mathrm{E}}S}\sum_k\sum_l c_{ijkl}\varepsilon_{kl} \\
& + \left[P_{ij}^{UNS}(1-r_{ij}) + P_{ij}^{BNS}(1-\delta)\right](1-M)\alpha_{ij}^{A}\beta_{ij}^{BV_{\mathrm{E}}S}\sum_k\sum_l c_{ijkl}\varepsilon_{kl} \\
& + \left\{P_{ij}^{UV_{\mathrm{I}}S}[r_{ij} + (1-r_{ij})M] + P_{ij}^{BV_{\mathrm{I}}S}[\delta + (1-\delta)M]\right\}\left(1-\alpha_{ij}^{U}\right)\beta_{ij}^{UV_{\mathrm{I}}S}\sum_k\sum_l c_{ijkl}\varepsilon_{kl} \\
& + \left\{P_{ij}^{UV_{\mathrm{I}}S}[r_{ij} + (1-r_{ij})M] + P_{ij}^{BV_{\mathrm{I}}S}[\delta + (1-\delta)M]\right\}\alpha_{ij}^{U}\beta_{ij}^{UV_{\mathrm{E}}S}\sum_k\sum_l c_{ijkl}\varepsilon_{kl} \\
& + \left[P_{ij}^{UV_{\mathrm{I}}S}(1-r_{ij}) + P_{ij}^{BV_{\mathrm{I}}S}(1-\delta)\right](1-M)\left(1-\alpha_{ij}^{A}\right)\beta_{ij}^{BV_{\mathrm{I}}S}\sum_k\sum_l c_{ijkl}\varepsilon_{kl} \\
& + \left[P_{ij}^{UV_{\mathrm{I}}S}(1-r_{ij}) + P_{ij}^{BV_{\mathrm{I}}S}(1-\delta)\right](1-M)\alpha_{ij}^{A}\beta_{ij}^{BV_{\mathrm{E}}S}\sum_k\sum_l c_{ijkl}\varepsilon_{kl} \\
& + \left\{P_{ij}^{UV_{\mathrm{E}}S}[r_{ij} + (1-r_{ij})M] + P_{ij}^{BV_{\mathrm{E}}S}[\delta + (1-\delta)M]\right\}\beta_{ij}^{UV_{\mathrm{E}}S}\sum_k\sum_l c_{ijkl}\varepsilon_{kl} \\
& + \left[P_{ij}^{UV_{\mathrm{E}}S}(1-r_{ij}) + P_{ij}^{BV_{\mathrm{E}}S}(1-\delta)\right](1-M)\beta_{ij}^{BV_{\mathrm{E}}S}\sum_k\sum_l c_{ijkl}\varepsilon_{kl}.
\end{aligned} \tag{15}$$

According to the previous assumption, equation (15) can be transformed into Eq. (16)

$$\begin{aligned}
\mu\varepsilon_{ij} = {} & \left[\left(P_{ij}^{UNS}\varphi + P_{ij}^{BNS}\right)\beta_{ij}^{BNS} + \left(P_{ij}^{UV_{\mathrm{E}}S}\varphi + P_{ij}^{BV_{\mathrm{E}}S}\right)\beta_{ij}^{BV_{\mathrm{E}}S}\right. \\
& \left. + \left(P_{ij}^{UV_{\mathrm{I}}S}\varphi + P_{ij}^{BV_{\mathrm{I}}S}\right)\beta_{ij}^{BV_{\mathrm{I}}S}\right]\sum_k\sum_l c_{ijkl}\varepsilon_{kl}.
\end{aligned} \tag{16}$$

Further simplification can obtain

$$\begin{aligned}
\mu\varepsilon_{ij} = {} & \left[\left(P_{ij}^{UV_{\mathrm{I}}S}\varphi^2 + P_{ij}^{BV_{\mathrm{I}}S}\varphi + P_{ij}^{UNS}\varphi + P_{ij}^{BNS}\right)\tau_1\right. \\
& \left. + \left(P_{ij}^{UV_{\mathrm{E}}S}\varphi + P_{ij}^{BV_{\mathrm{E}}S}\right)\varphi\tau_2\right]\beta\sum_k\sum_l c_{ijkl}\varepsilon_{kl},
\end{aligned} \tag{17}$$

where

$$\tau_1 = H\left(\frac{\sum_{j=1} P_j^{\mathrm{I}}(t)}{k_i(t)} - \gamma f_i\right), \quad \tau_2 = H\left(\frac{\sum_{j=1} P_j^{\mathrm{I}}(t)}{k_i(t)} - f_i\right).$$

Next, we can rewrite Eq. (17) as

$$\begin{aligned}
\sum_{k,l}\left\{\left[\left(P_{ij}^{UV_{\mathrm{I}}S}\varphi^2 + P_{ij}^{BV_{\mathrm{I}}S}\varphi + P_{ij}^{UNS}\varphi + P_{ij}^{BNS}\right)\tau_1\right.\right. \\
\left.\left. + \left(P_{ij}^{UV_{\mathrm{E}}S}\varphi + P_{ij}^{BV_{\mathrm{E}}S}\right)\varphi\tau_2\right]c_{ijkl} - \frac{\mu}{\beta}\xi_{ijkl}\right\}\varepsilon_{kl} = 0,
\end{aligned} \tag{18}$$

where ξ_{ijkl} presents the elements of the unital matrix. Let each element of the matrix O be

$$\begin{aligned}
o_{ijkl} = {} & \left[\left(P_{ij}^{UV_{\mathrm{I}}S}\varphi^2 + P_{ij}^{BV_{\mathrm{I}}S}\varphi + P_{ij}^{UNS}\varphi + P_{ij}^{BNS}\right)\tau_1\right. \\
& \left. + \left(P_{ij}^{UV_{\mathrm{E}}S}\varphi + P_{ij}^{BV_{\mathrm{E}}S}\right)\varphi\tau_2\right]c_{ijkl},
\end{aligned}$$

and $\Lambda_{\max}(O)$ be the greatest eigenvalue of the matrix O. By solving for variable in Eq. (18), the prevalence threshold of

our UBU–$NV_EV_IV_E$–SIS model is acquired as

$$\beta_c = \beta_c^B = \frac{\mu}{\Lambda_{\max}(O)}. \tag{19}$$

It is clear from Eq. (19) that, the threshold value β_c^B is closely related to the information dissemination process, immune measures taking process, recovery probability μ during epidemic transmission, the level of attenuation of infection rate φ, individual physical fitness condition f_{ij}, and physical fitness decline degree γ.

4. Numerical simulations

The following experiments were all completed on MATLAB software, and MC simulations have been used to validate the feasibility of the model proposed in this paper based on MMCA. Then, the influence of each parameter on the percent of the people infected with epidemics and infective threshold value were studied in turn. The original nodes value for the three layers is a random number between 5 and 30, and an initial social network with 1000 nodes is randomly generated according to the evolution process of the hypernetwork. In addition, let the starting value of the individual density of the state B, V_E, I to be $\rho^B = \rho^{V_E} = \rho^I = 0.1$. In the process of information diffusion, news with official background is often interpreted confrontationally by the public, and the phenomenon of "Tacitus trap" is gradually increasing.[45] Therefore, this paper assumes that the probability of an individual accepting clarifying information M is 0.3, and the probability of information forgetting δ is 0.1. The other parameters are set as follows: $\lambda = 0.5$, $\delta = 0.1$, $\theta = 0.2$, $\zeta = 0.5$, $\alpha = 0.6$, $\gamma = 0.5$, $\varphi = 0.6$, $\mu = 0.3$, $\mu_1 = \mu_2 = 0.4$, $\sigma_1 = \sigma_2 = 0.2$ (unless otherwise specified, the parameter settings in the next section are the same).[37,38,43,45,46]

First, we studied the influence of clarification intensity of official media M on epidemic threshold β_C and infection scale ρ^I. Figure 5 clearly shows that ρ^I decreases and β_C increases as M increases. This experimental result is consistent with reality, i.e., the trend of evolution indicates that the more the official media clarifies unverified information, the more people are inclined to disbelieve negative information, thus reducing the spread. Furthermore, people adopt more immune behaviors, resulting in a decrease in the number of infections and an increase in the threshold for epidemic outbreaks. Moreover, figure 6 provides an illustration of the impact of clarification intensity of official media M and the infection probability β on the scale of disease infection ρ^I for different initial negative information dissemination rates λ. By Figs. 6(a)–6(c) comparisons show that the increase of negative information dissemination rates λ can increase ρ^I and decrease β_C. In other words, it plays an important role to release the timely clarification of unverified false information by the media to weaken the diffusion of rumors in curbing the spread of the epidemic. Therefore, the whole society should boost the operation effectiveness of state-controlled media, increase the promotion of scientific publicity among citizens, and reduce the probability of initial belief in false information, to help epidemic prevention and control.

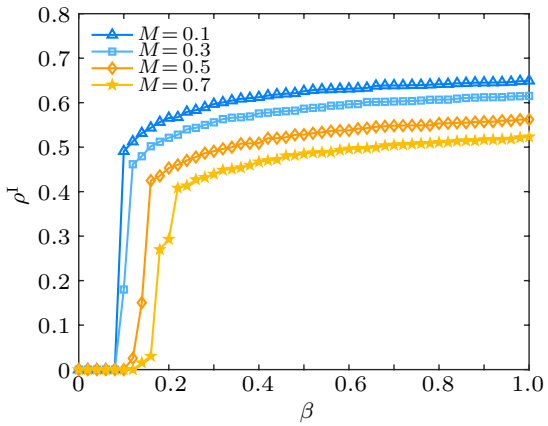


Fig. 5. The ρ^I as a function of the infection probability β under different clarification strengths of mass media M.

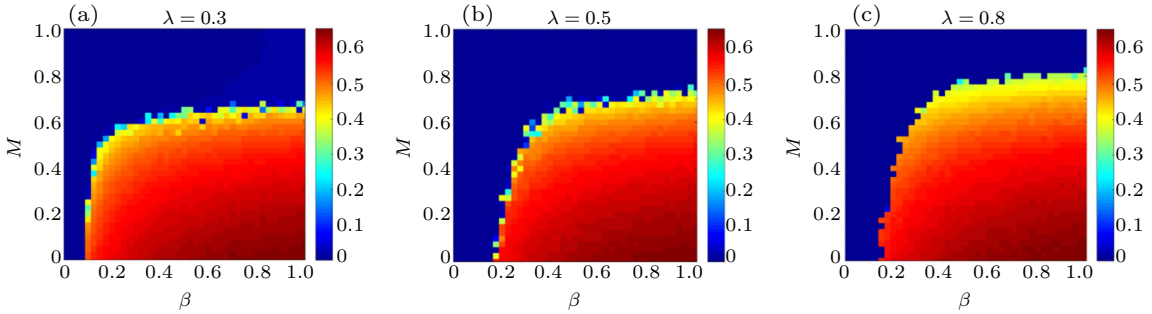


Fig. 6. The ρ^I as a function of the infection probability β and the clarification strength of mass media M. Setup λ from left to right as 0.3, 0.5, 0.8.

Figure 7 tests the influence of individual subjective acceptance doorsill θ on β_C and ρ^I. It is evident that as the magnitude of θ increases, the magnitude of ρ^I concomitantly rises, while the magnitude of β_C decreases. This evolutionary trend is consistent with the fact that when an individual's doorsill of acceptance of immune measures is extensive, they are less inclined to engage in immune behavior, thereby increasing the risk of contagion. Moreover, when the threshold for

acceptance was lower, they had almost the same proportion of infected individuals. When the infection rate β is large, the effect of θ on ρ^{I} is very slight. Moreover, figure 8 provides an illustration of the impact of individual subjective acceptance doorsill θ and the infection probability β on the scale of disease infection ρ^{I} for different initial behavior probability α. The infection rate that an individual can bear gradually increases, and the density of infectors is comparatively few with the increase of initial behavior probability α. Hence, in the prophase of the disease, timely promotion of relevant knowledge and other activities can reduce the threshold of public acceptance of immunization measures and increase the rate of citizens' adoption of immunization action, which can timely control the epidemic outbreak.

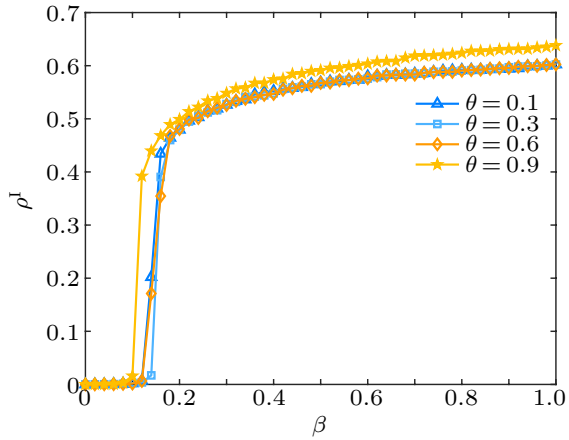


Fig. 7. The ρ^{I} as a function of the infection probability β under different individual subjective acceptance doorsill θ.

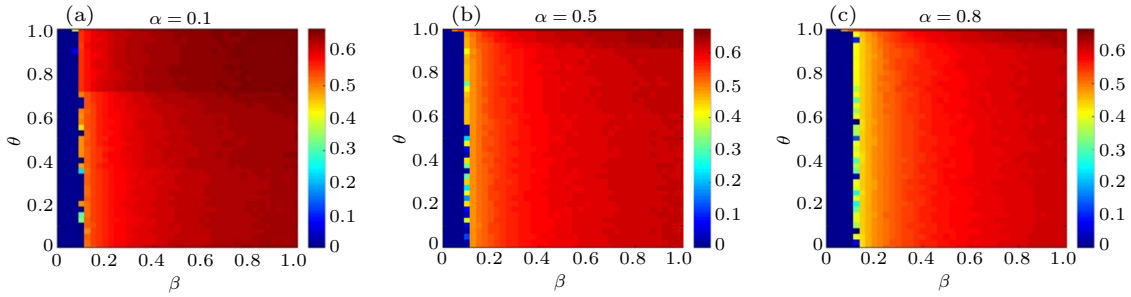


Fig. 8. The ρ^{I} as a function of the infection probability β and the individual subjective acceptance doorsill θ. Setup α from left to right as 0.2, 0.5, 0.8.

Then, we discuss the implication of the attenuation factor γ of individual immunity caused by failure to make immune operation on β_{C} and ρ^{I}. It is not difficult to observe in Fig. 9 that the increase of γ could raise the infection rate threshold value β_{C}, because increasing γ means increasing the physical fitness of individuals who are not engaged in immune behaviors or fail to be immune, and reducing the spread of infectious diseases by improving their physical fitness. What is more, figure 9 reveals that regardless of the value of γ, ρ^{I} remains in a stable state when β is approximately greater than 0.25. Thus, society should call on citizens to take immunization measures in time before the outbreak of the epidemic, and improve their own immune ability to lower down the epidemic scope of disease. Moreover, figure 10 provides an illustration of the impact of attenuation factor γ and the infection probability β on the scale of disease infectionρ^{I} for different attenuation factors of infection probability ϕ. The infected size ρ^{I} will be lower when ϕ is lower by comparing the three subgraphs in Fig. 10. This also confirms that when individuals disbelieve false messages or choose to take immunization measures to protect themselves, the risk of infection of the epidemic can be reduced, so then inhibiting its spread.

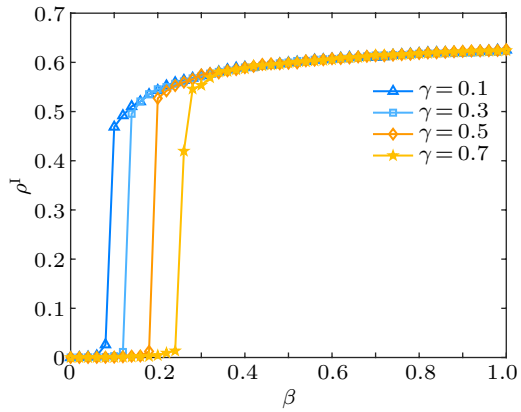


Fig. 9. The ρ^{I} as a function of the infection probability β under different attenuation factors of individual immunityγ. Set $M = 0.2$.

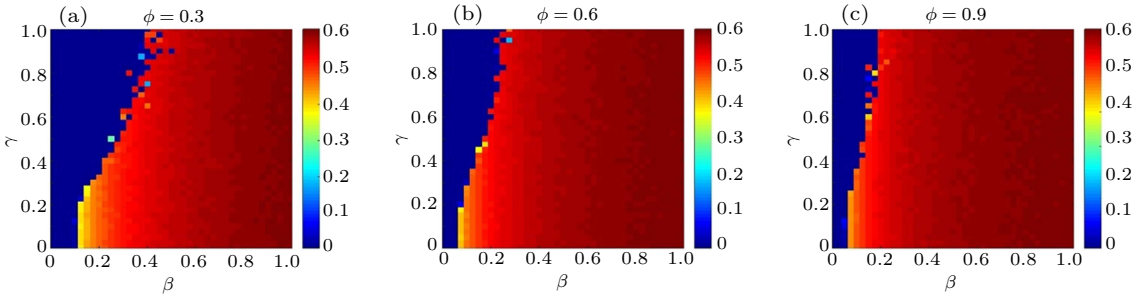


Fig. 10. The ρ^{I} as a function of the infection probability β and the attenuation factor of individual immunity γ. Setup ϕ from left to right as 0.3, 0.6, 0.9. Set $M = 0.2$.

We continue to focus on the effects of attenuation factor of infection probability ϕ. ϕ can be understood as the degree of self-protection obtained by individuals who choose not to believe negative information or take immune measures. The smaller ϕ is, the larger the intensity of self-protection of individuals and the less likely they are to be infected with the virus. Figure 11 shows the same idea that ρ^{I} increases and β_{C} decreases with the increase of ϕ. Meanwhile, looking into Figs. 12(a)–12(c), the proportion of infected people ρ^{I} increased significantly with the decrease of the entire population's the mean value of body constitution μ_2. This suggests that if each of us is low in physical fitness, the chances of an individual's immune system being broken will increase. Consequently, everyone's physical exercise should be strengthened to enhance the average physical fitness of the whole society, and actively take self-protection measures to reduce the spread of the epidemic.

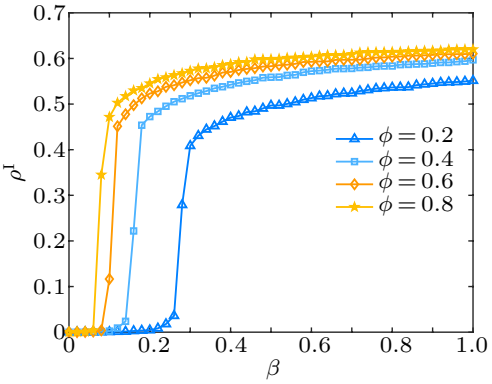


Fig. 11. The ρ^{I} as a function of the infection probability β under different attenuation factors of infection probability ϕ.

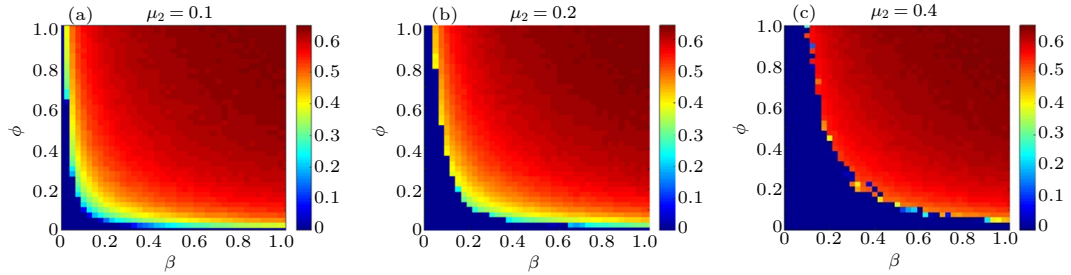


Fig. 12. The ρ^{I} as a function of the infection probability β and the attenuation factor of infection probability ϕ. Setup μ_1 from left to right as 0.1, 0.2, 0.4.

Finally, we also investigated the population's average self-discriminating ability μ_1 on β_{C} and ρ^{I}. As can be seen from Fig. 13, the prevalence threshold decreases effectively with the increase of μ_1. Specifically, β_{C} reaches its peak and tends towards a steady state when $\mu_1 = 0.7$. This is because, the accumulated average self-identification ability to a certain extent must lead to an improvement in the recognition abilities of the whole group by osmosis, and the possibility of trusting and spreading negative messages can be reduced, thereby affecting the adoption of immune behaviors and disease infection. In addition, figure 14 analyzes the impact of the fluctuation amplitude σ_1 of differences in self-discriminative ability on disease propagation. By comparisons, the larger σ_1, the larger share of group's affected people ρ^{I} . In other words, it is not only necessary to raise the average level of discriminability in the entire society, but also to pay more attention to enhancing the self-identification ability of individuals in the group, otherwise the difference in the group identification ability is too large, which will only make negative information more easily spread and have a greater impact on the spread of the epidemic. Thus, society should intensify the scientific knowledge education of the whole people, and improve the self-identification ability of the whole people while reducing the differences between individuals, which will do some benefit to preventing and controlling pandemic.

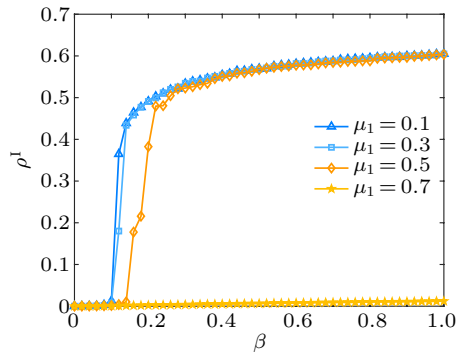


Fig. 13. The ρ^{I} and β_{c} as a function of the infection probability β under different population's average self-discriminating ability μ_1.

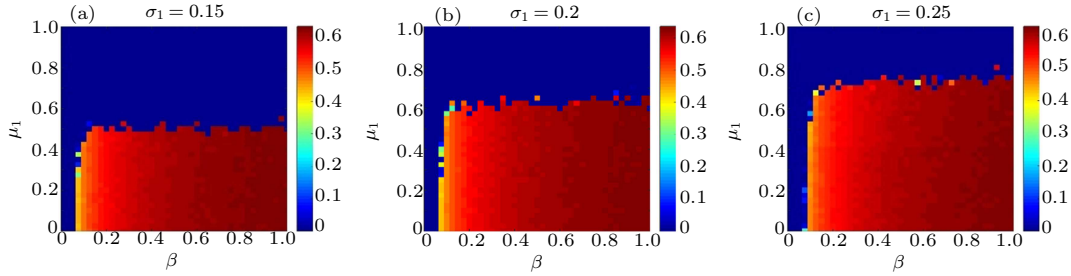


Fig. 14. The ρ^{I} as a function of infection probability β and the population's average self-discriminating ability μ_1. Setup σ_1 from left to right as 0.15, 0.2, 0.25.

5. Conclusion

This research probes the co-evolutionary effects of immune-relevant negative messages, immunization actions, and pandemic propagation by building a multi-layer dynamic super network UBU–$NV_{\mathrm{E}}V_{\mathrm{I}}V_{\mathrm{E}}$–$SIS$ model with official medium influence. Among them, the Heaviside step function has been brought in so as to describe the selection decision of three-layer processes. At the same time, factors such as self-identification ability and physical fitness are considered to improve the interaction between the networks. Firstly, theoretical analysis of the negative information diffusion, immunization behaviors inoculation, epidemic transmission process, and epidemic threshold is by applying the Micro Markov chain approach. Then, the validity of the above dynamic equations and theoretical results is confirmed by MATLAB numerical simulations. Finally, the impacts of parameters related to the co-evolution of mass media and three-layer networks on the scale and threshold of disease are discussed in turn through MMCA, and effective suggestions on how to control the spread of disease in social networks are put forward.

This paper describes the importance of disbelieving negative information and actively accepting and adopting immune conducts in dynamic hypernetworks for the spread of the epidemic, and several results were reached as follows: (i) Timely elimination of false negative information by official media through public relations can effectively weaken the spread of negative information and so then inhibit the spread of the epidemic. (ii) Negative messages increase the psychological resistance of individuals to immunization measures. The enhancement of self-identification ability to avoid bad information can push on individuals to take immune behaviors, thus reducing the risk of disease infection and suppressing the epidemic situation. (iii) Improving the physical fitness of individuals by adopting immune actions and daily exercise can raise the immune capacity of individuals, thereby reducing the possibility of being infected by diseases. (iv) Strengthening national education and fitness, narrowing the differences in ability between groups, and thus heightening the average self-discriminating ability and average physical fitness will have a positive effect on epidemic prevention and control.

Since the real network is dynamic, and the process of epidemic transmission is bound to be affected by negative information transmission and immunization behaviors inoculation, the epidemic transmission mechanism under the three-layer coupled network based on the evolution of the super-network is closer to the real situation, and can better predict the epidemic transmission in the real world. However, there are many factors affecting information transmission and immunization in social networks, and the actual dynamic network is more complex. In the future, we will propose models that take into account more influencing factors, try to gather realistic social network data to further confirm the authenticity of the model, or consider more dynamic evolutionary processes to complete the network environment.

References

[1] Jones K E, Patel N G, Levy M A, Storeygard A, Balk D, Gittleman J L and Daszak P 2008 *Nature* **451** 990
[2] Chala B and Hamde F 2021 *Frontiers in Public Health* **9** 715759
[3] Pertwee E, Simas C and Larson H J 2022 *Nat. Med.* **28** 456
[4] Apetrei C, Marx P A, Mellors J W and Pandrea I 2022 *Trends Microbiol* **30** 948
[5] Kermack W O and McKendrick A G 1927 *Proc. R. Soc. Lond. A* **115** 700
[6] Kermack W O and McKendrick A G 1991 *Bull. Math. Biol.* **53** 89
[7] Wang Z S, Guo Q T, Sun S W and Xia C Y 2019 *Appl. Math. Comput.* **349** 134
[8] Wang Z S, Xia C Y, Chen Z Q and Chen G R 2021 *IEEE Trans. Cybern.* **51** 1454
[9] Xia C Y, Wang Z S, Zheng C Y, Guo Q T, Shi Y T, Dehmer M and Chen Z Q 2019 *Inf. Sci.* **471** 185
[10] Huo L A and Wu B J 2024 *Chin. Phys. B* **33** 038702
[11] Li B X and Zhu L H 2024 *Information Processing & Management* **61** 103621
[12] Huang H, Chen Y H and Ma Y F 2021 *Appl. Math. Comput.* **388** 125536
[13] Zhou H, Ma Y H, Chen H Z and You X M 2024 *Commun. Nonlinear Sci. Numer. Simul.* **130** 107764
[14] Li D D, Xie W J and Han D 2024 *Appl. Math. Comput.* **474** 128700
[15] Kabir K M A and Tanimoto J 2019 *Commun. Nonlinear Sci. Numer. Simul.* **76** 92
[16] Lau J T F, Yeung N C Y, Choi K C, Cheng M Y M, Tsui H Y and Griffiths S 2009 *The BMJ* **339** b4164
[17] Wang J W, Xu W S, Chen W, Yu F Y and He J L 2021 *Physica -Stat. Mech. ITS Appl.* **583** 126281
[18] Zhang Y 2013 *Chaos, Solitons and Fractals* **56** 209
[19] Liu Y A and Wu B 2022 *Phys. Rev. E* **106** 034308
[20] Jovanovic R, Davidovic M, Lazovic I, Jovanovic M and Jovasevic-Stojanovic M 2021 *Int. J. Environ. Res. Public. Health* **18** 6217
[21] Meng X Y, Han S J, Wu L L, Si S B and Cai Z Q 2022 *Reliab. Eng. Syst. Saf.* **219** 108256
[22] Liu Y Y, Sanhedrai H, Dong G G, Shekhtman L M, Wang F, Buldyrev S V and Havlin S 2021 *Natl. Sci. Rev.* **8** nwaa229
[23] Li L, Dong G G, Zhu H P and Tian L X 2024 *Appl. Math. Comput.* **472** 128617
[24] Li C, Dai J Y and Li X 2024 *IEEE Trans. Comput. Soc. Syst.* **11** 2369
[25] Meng X Y, Lin J H, Fan Y F, Gao F J, Fenoaltea E M, Cai Z Q and Si S B 2023 *Chaos, Solitons and Fractals* **169** 113294
[26] Feng M Y, Li X X, Li Y H and Li Q 2023 *Chaos* **33** 043112
[27] Guo H L, Yin Q, Xia C Y and Dehmer M 2021 *Nonlinear Dyn.* **105** 3819
[28] Li C, Zhang Y A and Li X 2021 *IEEE Trans. Netw. Sci. Eng.* **8** 814
[29] Sha H Y and Zhu L H 2025 *Information Processing & Management* **62** 104016
[30] Wu B J and Huo L A 2024 *Chaos, Solitons and Fractals* **180** 114522
[31] Okita K, Tatsukawa Y, Utsumi S, Arefin M R, Hossain M A and Tanimoto J 2023 *Chaos, Solitons and Fractals* **167** 113029
[32] Yang P, Fan R G, Wang Y B and Zhang Y Q 2024 *Chin. Phys. B* **33** 070206
[33] Volpentesta A P 2008 *Eur. J. Oper. Res.* **188** 390
[34] Wang J W, Rong L L, Deng Q H and Zhang J Y 2010 *Eur. Phys. J. B* **77** 493
[35] Gong Y C, Wang M, Liang W, Hu F and Zhang Z K 2023 *Inf. Sci.* **644** 119284
[36] Wang J, Wang Z P, Yu P and Wang P W 2022 *Sustainability* **14** 13036
[37] Xie S J, Wang P W, Wang Z P and Zheng Y Y 2025 *IJICIC* **21** 617
[38] Huo L A and Yu Y 2023 *Chaos, Solitons and Fractals* **169** 113229
[39] Guo J L, Zhu X Y, Suo Q and Forrest J 2016 *Sci. Rep.* **6** 36648
[40] Yin Q, Wang Z S, Xia C Y and Bauch C T 2022 *Commun. Nonlinear Sci. Numer. Simul.* **109** 106312
[41] Zhao Y N and Jiang D Q 2014 *Appl. Math. Comput.* **243** 718
[42] Lv S, Wang Y, Guo C and Zhang L B 2024 *Nonlinear Dyn.* **112** 2367
[43] Yu P, Wang Z P, Sun Y N and Wang P W 2022 *Mathematics* **10** 4344
[44] Zhu L H, Ding Y and Shen S L 2025 *Mathematical Biosciences* **379** 109340
[45] Zhang J and Wang N 2024 *Expert Systems with Applications* **249** 123725
[46] Liu C, Guo M N, Chai Z L, Xin Z, Chen G J, Zimmet P Z and Yang J K 2023 *Diabetes Research and Clinical Practice* **201** 110723